

**CD39/ENTPD1 expression by CD4⁺Foxp3⁺ regulatory
T cells promotes hepatic metastatic tumor growth in mice**

XIAOFENG SUN,^{*,†} YAN WU,^{*,†} WENDA GAO,[‡] KEIICHI ENJOJI,^{*} EVA CSIZMADIA,^{*}
CHRISTA E. MÜLLER,[¶] TAKASHI MURAKAMI,[£] & SIMON C. ROBSON^{*,§}

Departments of ^{*}Medicine and [‡]Surgery, Transplantation Institute, Beth Israel
Deaconess Medical Center, Harvard Medical School, Boston, Massachusetts 02215,
USA; [¶]Pharmaceutical Institute, University of Bonn, Bonn 53121, Germany; [£]Division of
Bioimaging Sciences, Center for Molecular Medicine, Jichi Medical University,
Shimotsuke, Tochigi 329-0498, Japan

[†]These authors contributed equally to the work and surnames are arranged
alphabetically.

Running Title: CD39, Treg and metastatic tumors

Supplementary Materials

Supplementary Materials and Methods

***In vivo* Angiogenesis Assay**

In vivo angiogenesis was performed, as previously described.¹ Briefly, Rag1^{-/-} mice were adoptively transferred with wt (1×10^6) or Cd39 null CD4⁺ T cells (1×10^6). Twenty four (24) hrs later, mice were injected subcutaneously with 0.2 ml of a mixture of Growth Factor Reduced Matrigel (BD Bioscience), 500 nM SPP (Biomol International Inc., Plymouth Meeting, PA), 1.4 μ g/ml vascular endothelial growth factor (VEGF), 17.5 μ g/ml fibroblast growth factor (FGF)-2 and 116 μ g/ml BSA (fatty acid-free). Animals were euthanased on day 14. Matrigel plugs were harvested, snap-frozen and stored at -80°C before sectioning and immunohistochemical staining.

Plasma Chemistry

Plasma ALT, AST and BUN concentrations were measured by an automated autoanalyzer (Roche Mira Series, Global Medical Instrumentation Inc., Ramsey, MN).

Supplementary Figure Legends

Supplementary Figure 1. Melanoma tumor growth studies in mice post bone marrow transplantation (BMT). (A) Tumor volumes at day 14 post portal vein infusion of 1.5×10^5 luc-B16/F10 cells. (B) Representative images of tumor-bearing livers on day 14 (top) and *in vivo* bioluminescent imaging of tumor metastasis (bottom). (C) Representative immunohistochemical staining using anti-CD31 antibody and TUNEL staining (TdT) detecting apoptosis in livers of tumor-bearing mice (Magnification x200). Data are given as mean \pm SEM. * $P = .079$, ** $P = .006$.

Supplementary Figure 2. Analyses of tumor-infiltrating cells. (A) Representative immunohistochemical analyses performed on sections from melanoma-bearing wtBM-null mouse livers at day 10, staining as indicated for markers of T cells, monocyte-macrophages and myeloid suppressor cells as well as CD39 and Foxp3. (Magnification x200; except for Foxp3 x400). (B) Representative flow cytometric analyses of tumor-infiltrating mononuclear cells obtained from melanoma-bearing wt mice: left, gated on whole lymphocytes; right, gated on NK1.1⁺ cells. (C) Representative flow cytometry of tumor-infiltrating mononuclear cells from melanoma-bearing mice: gated on CD4⁺ cells. (D) Representative flow cytometry of tumor-infiltrating mononuclear cells from colonic tumor-bearing mice: gated on CD4⁺ cells. Numbers in quadrants indicate percent cells in the designated gates.

Supplementary Figure 3. CD39 expression on CD4⁺ T cells does not impact angiogenesis in immunodeficient mice *in vivo*. Freshly sorted wt CD4⁺ (1×10^6) or null CD4⁺ (1×10^6) T cells were adoptively transferred into Rag1^{-/-} mice at day 0, followed by 0.2 ml of Matrigel s.c. injection into left and right flanks. Matrigel plugs were then

harvested on day 14. Mice received PBS served as controls. Representative immunohistochemical staining on frozen sections of Matrigel plugs using anti-CD31 antibody to demonstrate endothelium (Magnification x200).

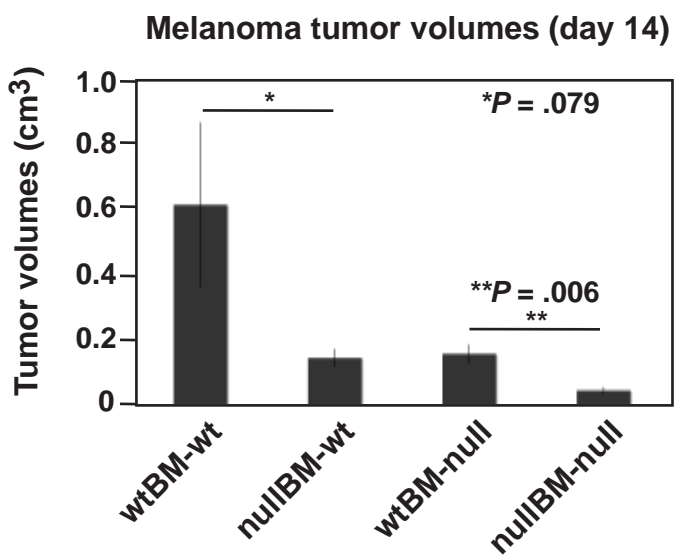
Supplementary Figure 4. NK cells are associated with colon cancer immune responses. (A) Representative liver images of tumor-bearing Rag1^{-/-} and (γc)/Rag2^{-/-} mice at day 10 post portal vein infusion of 1×10^5 MCA38 cells. (B) Tumor volumes of colonic tumor-bearing Rag1^{-/-} and (γc)/Rag2^{-/-} mice on day 10. (C) Absolute NK cell numbers in colonic tumor-bearing livers above. (D) Representative immunohistochemical staining using anti-NKp46 antibody on colonic tumor-bearing livers of (B) (Magnification x200). Data are given as means \pm SEM. * $P < 1E-06$.

Supplementary Figure 5. Hepatic and renal morphology and blood tests post administration of POM-1. Liver and kidney sections together with plasma were obtained from mice, as described above; Figure 7B and text. (A) Representative H&E staining of liver and kidney sections. Magnifications are shown on the bottom. (i-iii) tumor-bearing liver tissues; (iv-vi) tumor-adjacent liver tissues; (vii-ix) kidney tissues. (B) Tests of liver injury (ALT and AST) with different POM-1 doses. (C) Tests of renal function (BUN) as per (B). Plasma samples obtained from tumor-free wt and Cd39 null mice were used as controls. Data are given as means \pm SEM.

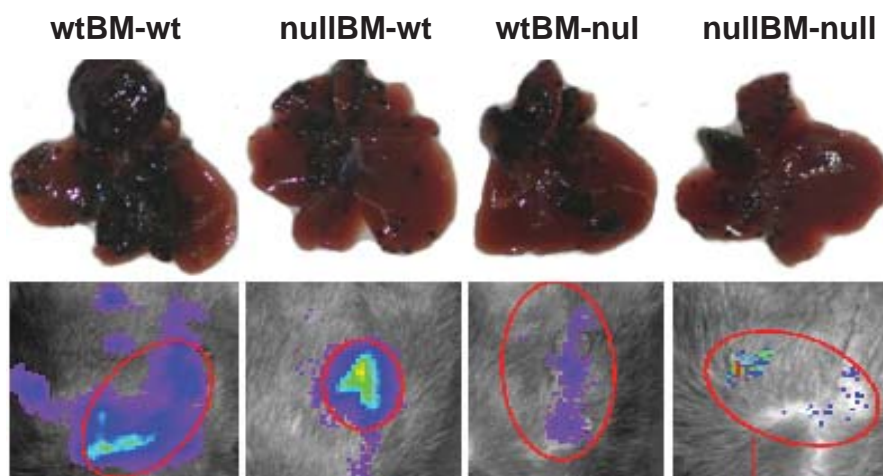
Supplementary References

1. Goepfert C, Sundberg C, Sévigny J, Enjyoji K, Hoshi T, Csizmadia E, Robson S. Disordered cellular migration and angiogenesis in cd39-null mice. *Circulation* 2001;104:3109-15.

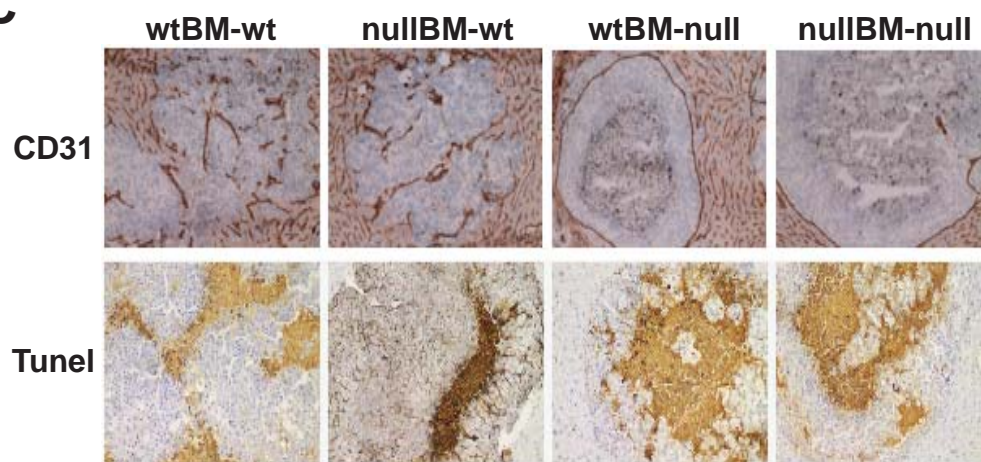
A



B

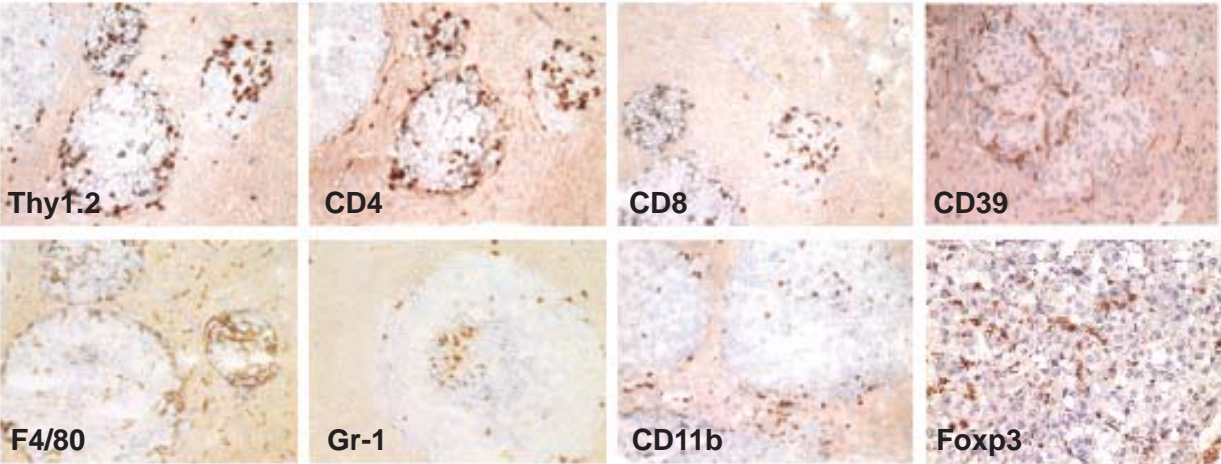


C

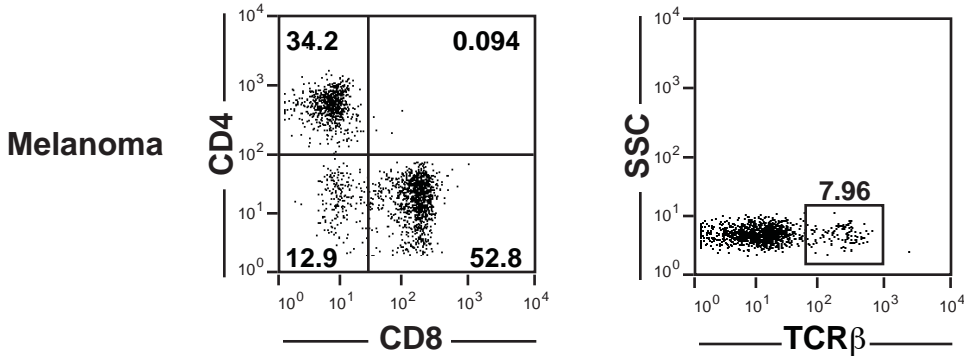


Supplementary Figure 2

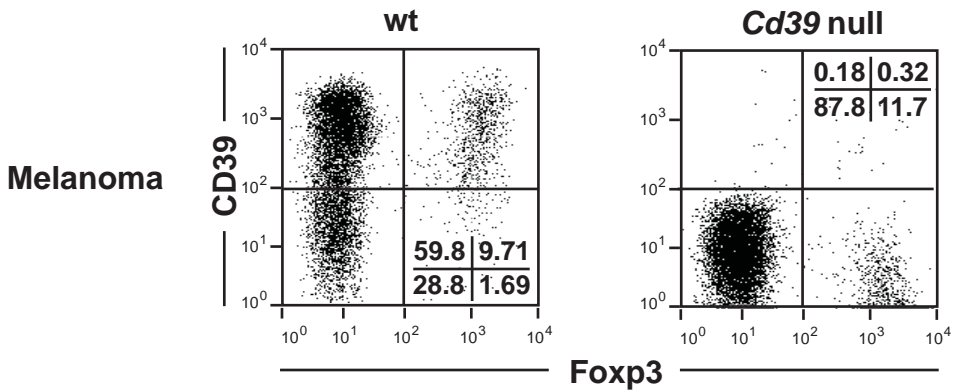
A



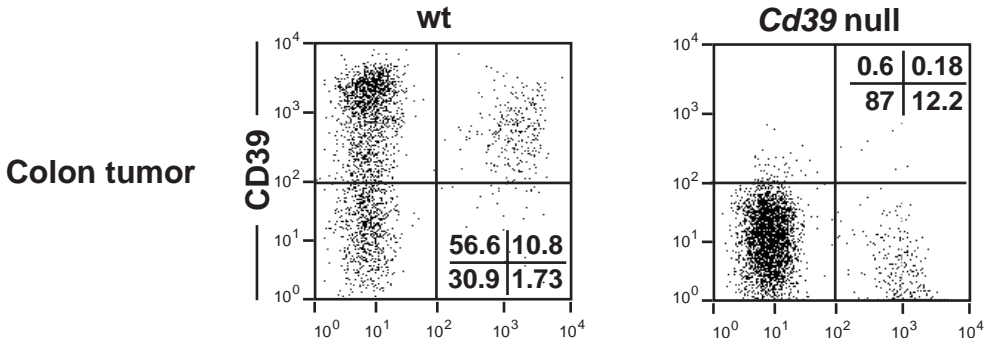
B



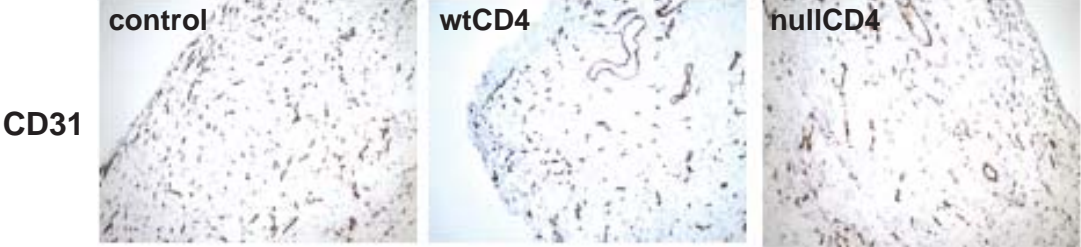
C



D



Supplementary Figure 3

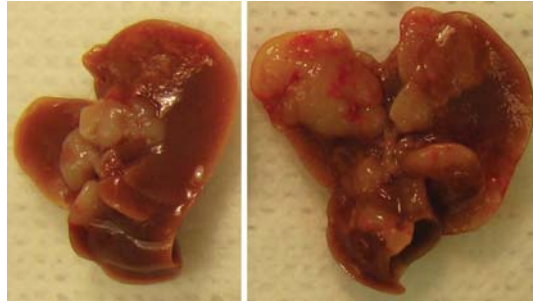


A

Colonic tumor metastasis (day 10)

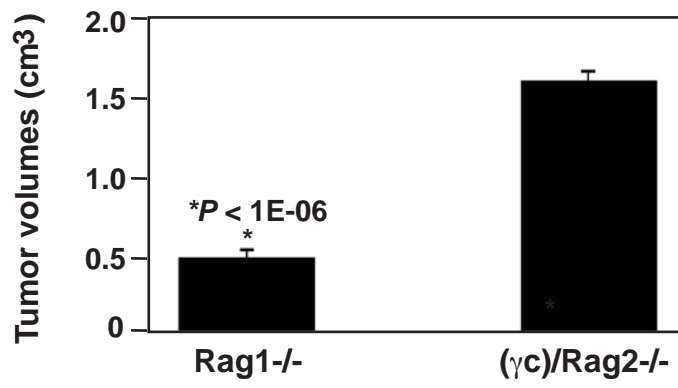
Rag1^{-/-}

(γ c)/Rag2^{-/-}

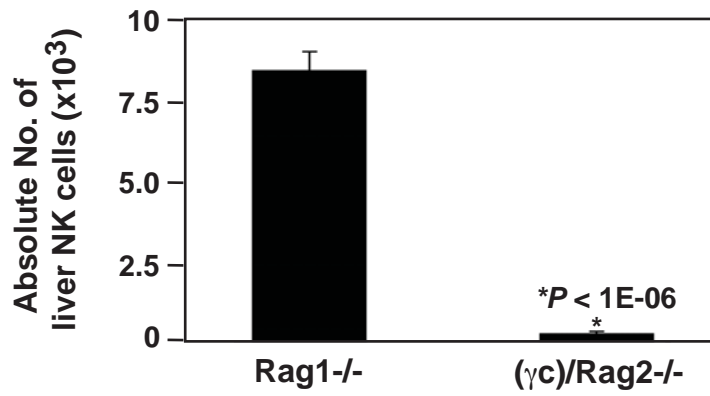


B

Colonic tumor volumes (day 10)



C

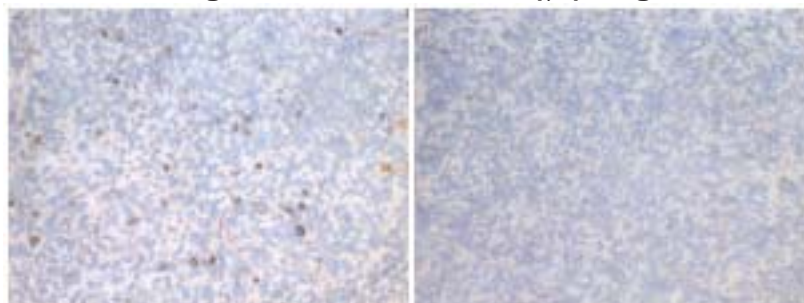


D

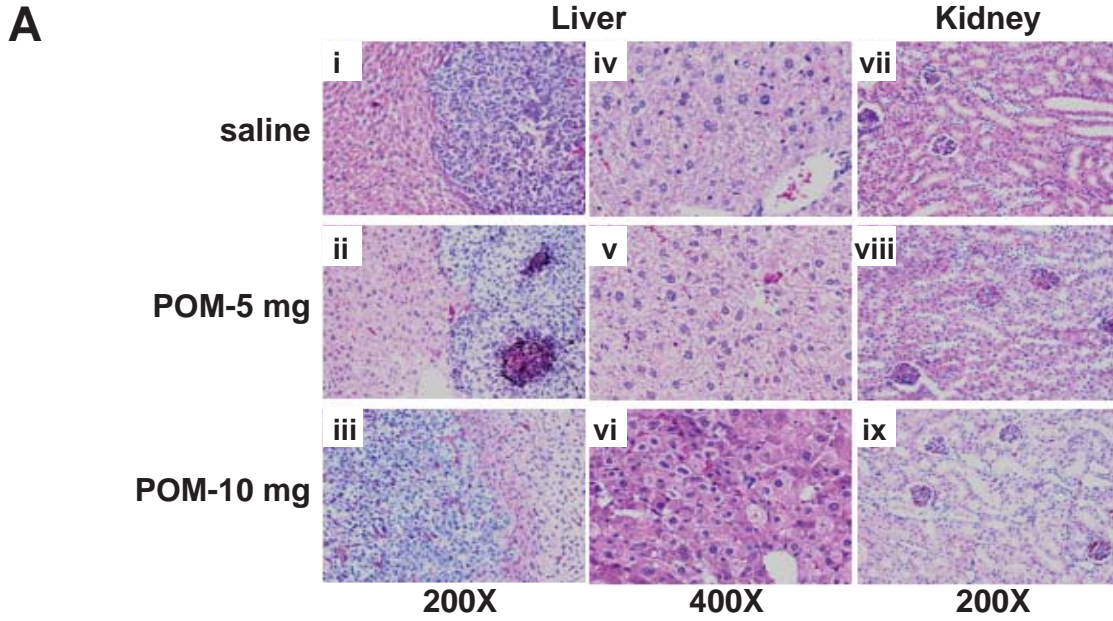
Rag1^{-/-}

(γ c)/Rag2^{-/-}

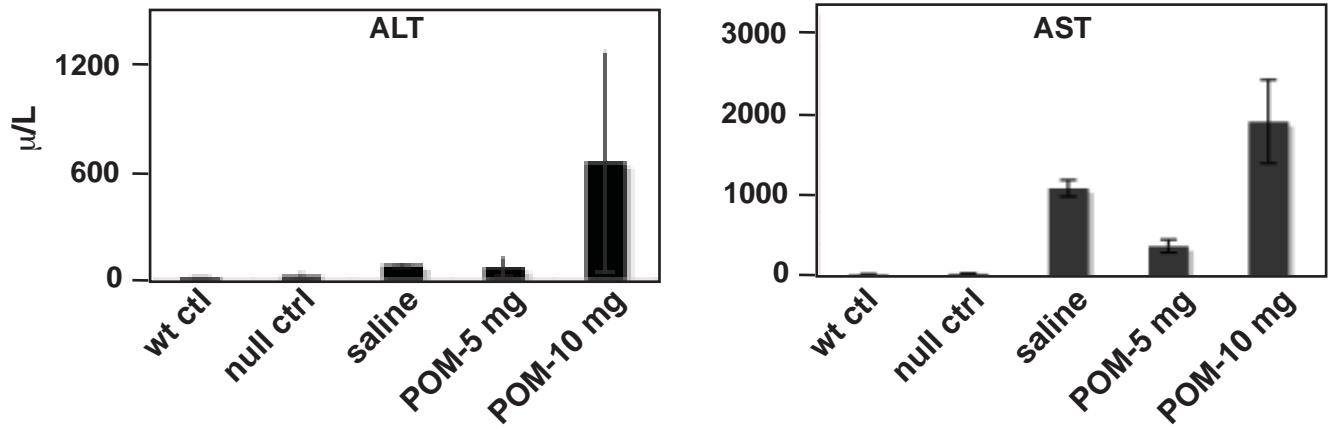
NKp46



Supplementary Figure 5



B Liver function tests



C Renal function tests

